



# 1 **High greenhouse gas fluxes from peatlands under various** 2 **disturbances in the Peruvian Amazon**

3  
4 Jaan Pärn<sup>1</sup>, Kaido Soosaar<sup>1</sup>, Thomas Schindler<sup>1,2</sup>, Katerina Machacova<sup>1,2</sup>, Waldemar Alegría  
5 Muñoz<sup>3</sup>, Lizardo Fachín<sup>4</sup>, José Luis Jibaja Aspajo<sup>3</sup>, Robinson I. Negron-Juarez<sup>5</sup>, Martin  
6 Maddison<sup>1</sup>, Jhon Rengifo<sup>4</sup>, Danika Journeth Garay Dinis<sup>3</sup>, Adriana Gabriela Arista Oversluijs<sup>3</sup>,  
7 Manuel Calixto Ávila Fucos<sup>3</sup>, Rafael Chávez Vásquez<sup>3</sup>, Ronald Huaje Wampuch<sup>3</sup>, Edgar Peas  
8 García<sup>3</sup>, Kristina Sohar<sup>1</sup>, Segundo Cordova Horna<sup>3</sup>, Tedi Pacheco Gómez<sup>3</sup>, Jose David Urquiza  
9 Muñoz<sup>3,6</sup>, Rodil Tello Espinoza<sup>3</sup>, and Ülo Mander<sup>1,2</sup>

10 <sup>1</sup> Department of Geography, Institute of Ecology and Earth Sciences, University of Tartu, Estonia  
11 (jaan.parn@ut.ee)

12 <sup>2</sup> Department of Ecosystem Trace Gas Exchange, Global Change Research Institute of the Czech Academy of  
13 Sciences, Brno, Czech Republic

14 <sup>3</sup> School of Forestry, National University of the Peruvian Amazon (UNAP), Iquitos, Peru

15 <sup>4</sup> Peruvian Amazon Research Institute (IIAP), Iquitos, Peru

16 <sup>5</sup> Lawrence Berkeley National Laboratory, Berkeley, CA, USA

17 <sup>6</sup> Max-Planck Institute for Biogeochemistry, Jena, Germany

18 *Correspondence to:* Jaan Pärn (jaan.parn@ut.ee)

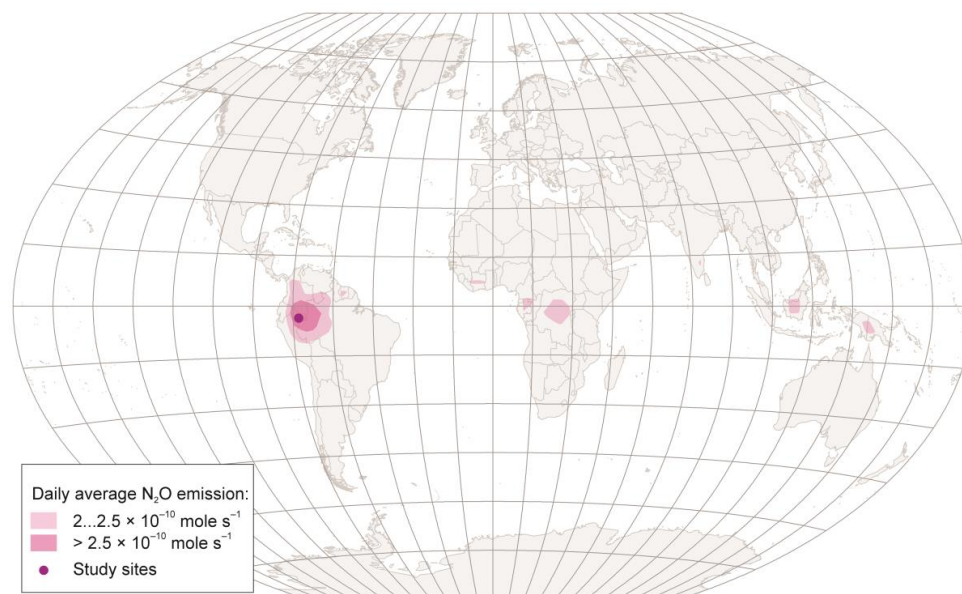
19 **Abstract.** Amazonian peat swamp forests remove large amounts of carbon dioxide (CO<sub>2</sub>) but anaerobic  
20 decomposition of the peat produces methane (CH<sub>4</sub>). Drought or cultivation cuts down on the CH<sub>4</sub> production but  
21 may increase the CO<sub>2</sub> emission. Varying oxygen content in nitrogen-rich peat produces nitrous oxide (N<sub>2</sub>O).  
22 Despite the potentially tremendous changes, greenhouse gas emissions from peatlands under various land uses  
23 and environmental conditions have rarely been compared in the Amazon. We measured CO<sub>2</sub>, CH<sub>4</sub> and N<sub>2</sub>O  
24 emissions from the soil surface with manual opaque chambers, and environmental characteristics in three sites  
25 around Iquitos, Peru from September 2019 to March 2020: a pristine peat swamp forest, a young forest and a  
26 slash-and-burn manioc field. The manioc field showed moderate peat respiration and N<sub>2</sub>O emission. The swamp  
27 forests under slight water table drawdown emitted large amounts of CO<sub>2</sub> and N<sub>2</sub>O while retaining their high CH<sub>4</sub>  
28 emissions. Most noticeably, a heavy shower after the water-table drawdown in the pristine swamp forest created  
29 a hot moment of N<sub>2</sub>O. Nitrifier denitrification was the likely source mechanism, as we rule out nitrification and  
30 heterotrophic denitrification. We base the judgement on the lack of both nitrate and oxygen, and the suppressed  
31 denitrification potential in the topsoil. Overall, our study shows that even moderate drying in Peruvian palm  
32 swamps may create a devastating feedback on climate change through CO<sub>2</sub> and N<sub>2</sub>O emissions.

## 33 **1 Introduction**

34 Peatlands are an enormous sink of carbon and nitrogen (IPCC, 2019). Natural and human disturbances may release  
35 them as greenhouse gases (GHG). The threat is particularly acute in tropical peatlands (IPCC, 2019). Amazonian  
36 swamp forests hold almost a half of tropical peatlands globally (Leifeld and Menichetti, 2018). Most of them are  
37 isolated from major population centres and roads, and thus inaccessible to logging and agriculture (Lilleskov et



38 al., 2019). Undisturbed peat swamp forests sequester carbon (C) for tens of kyr (Ruwaimana et al, 2020). Anoxic  
39 decomposition of peat under high water table yields methane (CH<sub>4</sub>; Teh et al., 2017; Hergoualc'h et al., 2020),  
40 and suboxic processes in nitrogen-rich peat under intermediate (50 to 60%) water content produce nitrous oxide  
41 (N<sub>2</sub>O; Melillo et al., 2001; Jauhainen et al., 2012; Rubol et al., 2012; Hu et al., 2015; Pärn et al., 2018;  
42 Hergoualc'h et al., 2020). The 5.4 million km<sup>2</sup> Amazon rainforest is the biggest hotspot of N<sub>2</sub>O in the world  
43 (Figure 1; Ricaud et al., 2009) emitting 1,300 Gg N<sub>2</sub>O-N yr<sup>-1</sup> (Melillo et al., 2001). The contribution of swamp  
44 forests to the hotspot is poorly known (van Lent et al., 2015; Guilhen et al., 2020) but a Peruvian palm peat swamp  
45 emitted 0.5 to 2.6 kg N<sub>2</sub>O-N ha<sup>-1</sup> yr<sup>-1</sup> (van Lent et al., 2015). This was similar to swamp forests of Southeast Asia  
46 that emit  $2.7 \pm 1.7$  kg N<sub>2</sub>O-N ha<sup>-1</sup> yr<sup>-1</sup> (average  $\pm$  standard deviation; van Lent et al., 2015). The major source  
47 mechanism behind N<sub>2</sub>O emissions is denitrification, as identified from N<sub>2</sub>O profiles and porewater nitrogen forms  
48 in wetting experiments on intact soil cores (Butterbach-Bahl et al., 2013; Liengaard et al., 2014; Hu et al., 2015).  
49 N<sub>2</sub>O is an intermediate product of denitrification in either suboxic soil or under varying oxygen availability both  
50 in time and between anoxic soil aggregates and air-filled pores (Butterbach-Bahl et al., 2013; Hu et al., 2015).  
51 Only after depletion of nitrate (NO<sub>3</sub><sup>-</sup>) is N<sub>2</sub>O reduced to inert N<sub>2</sub> (Liengaard et al., 2014). However, the Amazon  
52 has an exceptionally high 10% share of nitrification in N<sub>2</sub>O production (Inatomi et al., 2019). In a Peruvian palm  
53 peat swamp forest, Hergoualc'h et al. (2020) identified nitrifier denitrification as the probable source process for  
54 the high N<sub>2</sub>O emission. Brazil is also a major contributor to the global increase in N<sub>2</sub>O emissions during the last  
55 decades, owing to the increase in nitrogen (N) fertilisation (Thompson et al., 2019).



56

57 **Figure 1: Global hotspots of N<sub>2</sub>O emission measured in upper troposphere by IASI satellite (Ricaud et al., 2009), and**  
58 **location of study sites.**

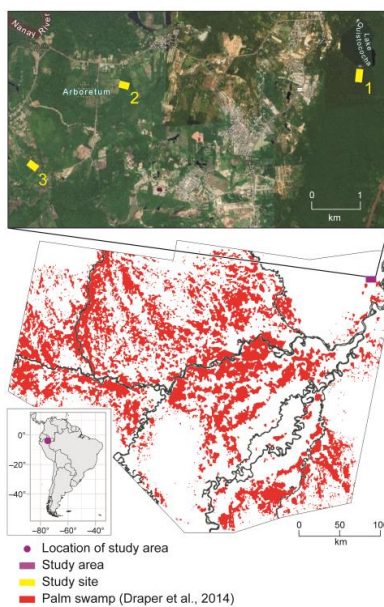
59 C sequestration dominates the GHG balance in natural peat swamps (Frolking and Roulet, 2009) whereas  
60 disturbances increase GHG emissions (Turetsky et al., 2015; IPCC, 2019). In the Amazon, drought is a quickly  
61 increasing disturbance which is shortening the growth period and imposing tree decline (IPCC, 2019). Droughts  
62 increase ecosystem respiration. Microbes that respire much of the CO<sub>2</sub> rapidly acclimatise with the rising



63 temperature which may send the ecosystems down a positive feedback loop (Karhu et al., 2014). Thus, drought-  
64 induced tree mortality is saturating the Amazon C sink (Hubau et al., 2020).  
65 The studies made on mineral soil are unreliable for the climate-change effects on peat swamps. In contrast to  
66 mineral soils, water table stays above or near the ground in peat swamps throughout the dry season, making the  
67 carbon and nitrogen stocks resistant (Turetsky et al., 2015). On the other hand, peatland clearing, commonly with  
68 fire, renders the peat carbon and nitrogen stocks vulnerable (Turetsky et al., 2015; Lilleskov et al., 2019).  
69 However, few studies have compared greenhouse gas fluxes across a variety of land uses and water tables in  
70 Amazonian peat swamps. To fill the knowledge gap, we set an objective to identify environmental drivers of CO<sub>2</sub>,  
71 CH<sub>4</sub> and N<sub>2</sub>O fluxes across gradients of land use and water table, we held a measurement campaign around Iquitos,  
72 the Peruvian Amazon.

## 73 2 Material and Methods

74 We observed fluxes of the three GHGs using opaque soil chambers and measured potential environmental factors  
75 in three current or former *Mauritia flexuosa* palm dominated swamps under various disturbance histories (Figure  
76 2): 1 — “Swamp”, a natural forest in the Quistococha lake floodplain (6 m peat; see Roucoux et al., 2013 for  
77 detailed physical description) 3°50'03.9" S, 73°19'08.1" W, 2 — “Slope”, a 12-year old secondary forest grown  
78 over a fallow pasture and banana plantation on an alluvial toe slope (0.1 to 0.3 m peat) 3°50'10.7" S, 73°21'45.0"  
79 W and 3 — “Manioc”, a slash-and-burn manioc (*Manihot esculenta*) field (0.03 to 0.15 m peat), 3°51'00.0" S,  
80 73°22'45.8" W.



81  
82 **Figure 2: Location of study sites (1 – Swamp, 2 – Slope, and 3 – Manioc) and distribution of palm swamp forests in the**  
83 **Pastaza-Marañon Basin (data from Draper et al., 2014). Background image for the site location map above © Google**  
84 **Maps.**

85 On the Slope and Manioc sites, we established three topequivalent stations at an interval of 15 m. Each station  
86 received three chambers three to five meters apart from each other. CO<sub>2</sub>, CH<sub>4</sub> and N<sub>2</sub>O were sampled using the



87 static chamber method with PVC collars of 0.5 m diameter and 0.1 m depth installed in the peat. The inside of  
88 collars at the Slope site was covered with sparse < 0.2 m tall *Pteridaceae* ferns while the collars in the Swamp  
89 and Manioc sites contained no plants. We used white 65 L PVC truncated conical gas sampling chambers. We  
90 did not use extra cover against sunlight but the chamber design is generally regarded as opaque (Hutchinson and  
91 Livingston, 1993). They were placed into water-filled rings on the collars (Mander et al., 2014). Gas was sampled  
92 from chamber headspace into a pre-evacuated 50 mL glass vial every 20 minutes during a 1 h session (Hutchinson  
93 and Livingston, 1993). The sessions were held between 8 and 11 hours of daytime, to represent the average diurnal  
94 emissions (according to Figures 11 and 12 in Griffis et al., 2020). We conducted nine sampling sessions in the  
95 Swamp forest from September 2019 to March 2020, four sessions in the Slope forest in September 2020 and nine  
96 sessions in the Manioc field from September 2019 to March 2020 according to the schedule presented in Table 1.  
97 Before the first sampling in September, young manioc saplings had been planted. By 15 February, they had grown  
98 to 3 m height covering the whole field with a sparse canopy (> 30% shading). No manioc plant grew directly out  
99 of the stationary gas sampling collars at any time. The manioc was harvested in late February, leaving a bare field  
100 for the March sampling. The gas samples were transported to a laboratory at the University of Tartu and analysed  
101 by gas chromatography (GC-2014; Shimadzu, Kyōto, Japan) equipped with an electron capture detector for  
102 detection of N<sub>2</sub>O and a flame ionisation detector for CH<sub>4</sub>, and Lofffield-type autosamplers. An individual gas flux  
103 was determined on the basis of linear regression obtained from consecutive concentrations (Hutchinson and  
104 Livingston, 1993). A *p* level of < 0.05 was accepted for the goodness of fit to linear regression. Insignificant  
105 fluxes (*p* > 0.05) below the accuracy of gas chromatograph (regression change of gas concentration  $\delta v < 10$  ppb)  
106 were included in the analysis as zeros. Each station was equipped with a 1 m deep observation well (a 0.05 m  
107 perforated PP-HT pipe wrapped in filter textile). Water table height was recorded from the observation wells  
108 during the gas sampling. Soil moisture was measured with a GS3 sensor connected to a ProCheck handheld reader  
109 (Decagon Devices, Pullman, WA, USA). Soil temperature was measured between 0.1 to 0.4 m depth at an interval  
110 of 0.1 m. Soil oxygen (O<sub>2</sub>) content was measured with a stand-alone fibre optic oxygen meter (PreSens,  
111 Regensburg, Germany) at 0.05 m and 0.005 m depths in September and March.  
112



113 **Table 1: Time schedule of sampling sessions in the study sites. X marks one sampling session.**

Date	Swamp	Slope	Manioc
16.09.2019	X		
17.09.2019	X		
19.09.2019		XX	
20.09.2019		XX	
21.09.2019			XX
22.09.2019			XX
24.09.2019	X		
25.09.2019	X		
04.01.2020			X
11.01.2020	X		
18.01.2020			X
25.01.2020	X		
04.02.2020			X
08.02.2020	X		
15.02.2020			X
22.02.2020	X		
02.03.2020			X
03.03.2020			X
04.03.2020	X		

114

115 A peat sample of 150 to 200 g was collected from each chamber between 0 to 0.1 m depth after the sampling  
116 sessions in September and March. The soil samples were stored at 5 °C and transported under the same  
117 temperature to Estonian University of Life Sciences for chemical and physical analyses. At the laboratory, plant-  
118 available (KCl extractable) phosphorus (P) was determined on a FIAstar 5000 flow injection analyser (FOSS,  
119 Hilleroed, Denmark; Ruzicka and Hansen, 1981). Plant available potassium (K) was determined from the same  
120 solution by the flame-photometric method, and plant available magnesium (Mg) was determined from a 100 mL  
121 ammonium acetate solution with a titanium-yellow reagent on the flow injection analyser (Ruzicka and Hansen,  
122 1981). Calcium (Ca) was analysed using the same solution by the flame photometrical method (Ruzicka and  
123 Hansen, 1981). Soil pH was determined on a 1N KCl solution. Soil ammonium (NH<sub>4</sub><sup>+</sup>) and nitrate (NO<sub>3</sub><sup>-</sup>) contents  
124 were determined on a 2M KCl extract of soil by flow-injection analysis (Ruzicka and Hansen, 1981). Total N and  
125 C contents of oven-dry samples were determined using a dry combustion method on a varioMAX CNS elemental  
126 analyser. The soil organic matter (SOM) content of the oven-dry samples was determined by loss on ignition at  
127 360° C.

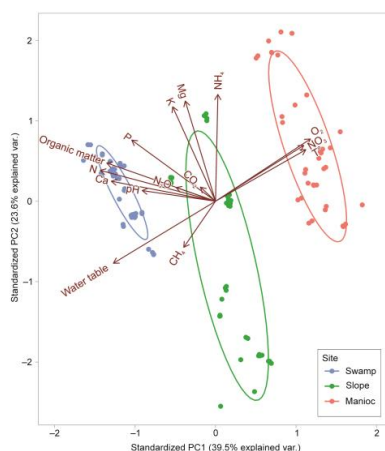
128 For use with the He–O<sub>2</sub> method at our University of Tartu laboratory, we collected intact soil cores (0.068 m  
129 diameter, 0.06 m height) from the top 0.1 m from each chamber after the last gas sampling sessions in September  
130 and March. The helium-atmosphere soil-incubation technique (Espenberg et al., 2018) was used to measure  
131 potential N<sub>2</sub>O and molecular nitrogen (N<sub>2</sub>) fluxes from soil cores in the same laboratory. The cylinders with the  
132 intact soil cores were placed into special gas-tight incubation vessels locating in the climate chamber. Gases were  
133 removed by flushing with an artificial gas mixture (21.0% O<sub>2</sub>, 358 ppm CO<sub>2</sub>, 0.313 ppm N<sub>2</sub>O, 1.67 ppm CH<sub>4</sub>,  
134 5.97 ppm N<sub>2</sub> and the rest He). The new atmosphere equilibrium by continuously flushing the vessel headspace  
135 with the artificial gas mixture at 20 mL per min was established after 12–24 h. The flushing time depended on the



136 soil moisture. The temperature was kept similar to the field temperature during the incubation. Concentrations of  
137  $\text{N}_2\text{O}$  and  $\text{N}_2$  were analysed by the GC-2014 (Shimadzu, Japan). Flux rates were calculated from the actual gas  
138 concentration of the continuous flow rate from the vessel headspace after subtraction of a blank value from a  
139 vessel without a soil core, which is equivalent to concentrations from the artificial  $\text{He}-\text{O}_2$  gas mixture.  
140 We tested normal distribution of the samples by the Kolmogorov–Smirnov and Shapiro–Wilk’s tests using the  
141 *stats* package in R. As data for most of the sites were not normally distributed ( $p > 0.05$ ), we analysed relationships  
142 between the GHG fluxes and environmental characteristics by the nonparametric generalised additive models  
143 (GAM) using the simplest smoothing term ( $k=3$ ) in the *mgcv* package in R, and principal component analysis  
144 (PCA) using the *stats* package in R. For each cluster of replicate measurements we plotted a normal data ellipse  
145 with size defined as a normal probability equal to 0.68. Significance of differences between sites was checked by  
146 the unpaired two-sided Wilcoxon rank sum test (the *wilcox.test* function, *stats* package in R).

### 147 3 Results and Discussion

148 The PCA clearly separated our three sites along a water table gradient closely followed by soil  $\text{O}_2$  content, soil  
149 temperature and  $\text{NO}_3^-$  content gradients (Figure 2). The waterlogged swamp peat did not contain a detectable  
150 amount of  $\text{NO}_3^-$ . No fertiliser was added according to our knowledge on our sites. Therefore, the high amount of  
151  $\text{NO}_3^-$  in the manioc field was probably produced by nitrification induced by the slash-and-burn and subsequent  
152 water-table drawdown. Within the sites, the PCA distinguished the gas-sampling chambers along a soil nutrient  
153 gradient (Ca, Mg, pH, P, total N,  $\text{NH}_4^+$ ) independent from the water table changes. The nutrients may have  
154 enhanced heterotrophic  $\text{CO}_2$  and  $\text{N}_2\text{O}$  production. Within-site differences in water table were still remarkable.  
155 The water table in the slope forest varied between  $-0.09$  and  $-0.13$  m at the wet station, between  $-0.115$  and  $-$   
156  $0.15$  m at the middle and around  $-0.7$  m at the dry station. The water table in the palm swamp varied from  $-0.12$   
157 to  $-0.085$  m in mid-September, rose to  $-0.03$  m after a 30 mm shower 6 hours before the 24 September session  
158 and dropped to  $-0.07$  m during the next dry day. From January to March, the water table in the palm swamp was  
159 steadily  $-0.03$  m. Soil  $\text{O}_2$  content remained  $< 0.1$   $\text{mg L}^{-1}$  at both 0.005 and 0.05 m depth throughout the  
160 observations in the Swamp forest.

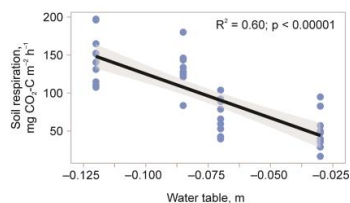


161

162 **Figure 3: Principal component analysis (PCA) of GHG fluxes and environmental characteristics in September 2019.**  
163 **Each data point represents one GHG flux replicate measurement. A normal data ellipse is shown around points from**  
164 **each site.**

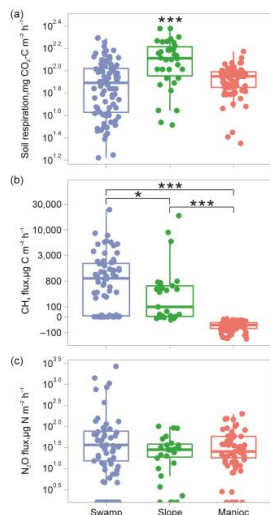


165 The dry station (water table  $-0.7$  m; soil water content  $0.26 \text{ m}^3 \text{ m}^{-3}$ ; soil temperature around  $26 \text{ }^\circ\text{C}$  at  $10 \text{ cm}$  depth)  
 166 of the young swamp forest respired the largest amount of  $\text{CO}_2$  (session averages of  $130$  to  $210 \text{ mg C m}^{-2} \text{ h}^{-1}$ ).  
 167 That station apparently represents the optimal moisture for soil respiration (Byrne et al., 2005; Balogh et al.,  
 168 2011). The respiration declined with the increase in the water table (session averages of  $43$  to  $91 \text{ mg C m}^{-2} \text{ h}^{-1}$  at  
 169 the wettest station). The similarly dry but hotter manioc field (soil water content  $0.15$  to  $0.24 \text{ m}^3 \text{ m}^{-3}$ ; soil  
 170 temperature  $26$  to  $34 \text{ }^\circ\text{C}$  at  $0.1 \text{ m}$  depth during all months) respired steadily  $75$  to  $98 \text{ mg C m}^{-2} \text{ h}^{-1}$  throughout the  
 171 study period (Figure 5a), regardless of the noticeable changes in manioc rooting, height and canopy from  
 172 September to March. The Swamp peat ( $\text{O}_2 < 0.1 \text{ mg L}^{-1}$  at both  $0.005$  and  $0.05 \text{ m}$  depth) respired  $49$  to  $150 \text{ mg C}$   
 173  $\text{m}^{-2} \text{ h}^{-1}$  as session average (Figure 5a) in negative linear relationship with water table. Although soil water content  
 174 remained above  $0.8 \text{ m}^3 \text{ m}^{-3}$  and soil  $\text{O}_2$  content stayed  $< 0.1 \text{ mg L}^{-1}$  at both  $0.005$  and  $0.05 \text{ m}$  depth from  $24$   
 175 September onward, the aerenchymous palm roots probably provided  $\text{O}_2$  in the deeper soil zones (van Lent et al.,  
 176 2019). Most of the respired C was offset in the gross primary production (GPP) of trees (as observed by the EC  
 177 technique above the canopy; Griffis et al., 2020). However, during the dry season of 2019 including the  
 178 September, ecosystem respiration of the whole Quistococha swamp forest increased and exceeded the  
 179 concurrently declining GPP by a steady average of  $600 \text{ mg C day}^{-1}$  (EC measured; Griffis et al., 2020). This shows  
 180 that peat respiration will prevail the C balance of the palm swamp during the dry season even when the peat  
 181 remains wet.



182

183 **Figure 4: Relationship between soil respiration and water table in the Swamp forest.**



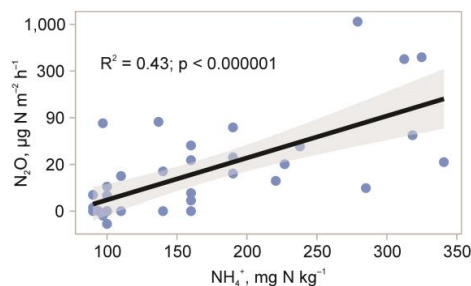
184

185 **Figure 5: Box plots of soil  $\text{CO}_2$  (a),  $\text{CH}_4$  (b) and  $\text{N}_2\text{O}$  (c) fluxes in study sites. Significant differences according to  
 186 Wilcoxon test are shown with asterisks as follows: \* –  $p < 0.05$ ; \*\* –  $p < 0.01$ ; \*\*\* –  $p < 0.001$ . Asterisks directly above  
 187 box without brackets denote significant difference from all other sites in the plot.**

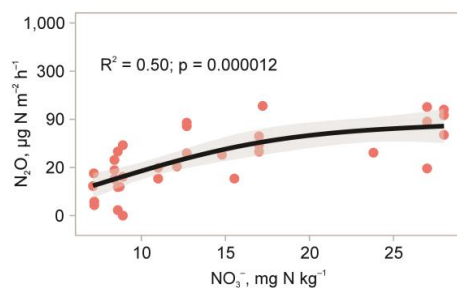


188 The wet swamp forest floor emitted session averages of 530 to 9,100  $\mu\text{g CH}_4\text{-C m}^{-2} \text{h}^{-1}$  (Figure 5b) owing to the  
189 high  $-0.03$  to  $-0.12$  m water table (Hergoualc'h et al., 2020). This lay within the range of  $\text{CH}_4$  fluxes reported  
190 from Brazilian flooded swamp forest soils (*igapo* and *varzea*; Pangala et al., 2017). The similarly high 2,000 to  
191 3,200  $\mu\text{g C m}^{-2} \text{h}^{-1}$  reported earlier from nearby peat swamp forest (Hergoualc'h et al., 2020), and the 600 to 1,300  
192  $\mu\text{g C m}^{-2} \text{h}^{-1}$  measured above the canopy with water table between  $-0.03$  and  $-0.12$  m (Griffis et al., 2020) show  
193 that even during the dry season the palm swamp emits a lot of  $\text{CH}_4$  and a large part of it reaches the atmosphere.  
194 The dry slash-and-burn manioc field consumed  $\text{CH}_4$  at a session mean rate of 49 to 83  $\mu\text{g C m}^{-2} \text{h}^{-1}$  (Figure 5b).  
195 The natural swamp peat produced session averages of 65 and 58  $\mu\text{g N}_2\text{O-N m}^{-2} \text{h}^{-1}$  during the 0.12–0.085 m  
196 water-table drawdown on 16 and 17 September, respectively. A 30 mm shower on the night before 24 September  
197 restored the water table to  $-0.03$  m, caused a 2-fold drop in peat respiration (Figure 4), and initiated session-  
198 average peaks of 360 and 420  $\mu\text{g N m}^{-2} \text{h}^{-1}$  from the 190 mg dry  $\text{kg}^{-1}$  soil  $\text{NH}_4^+\text{-N}$  on 24 and 25 September. During  
199 January to March, a steady average of 11.6  $\mu\text{g N m}^{-2} \text{h}^{-1}$  (session averages of 2.3 to 27  $\mu\text{g N m}^{-2} \text{h}^{-1}$ ) was produced  
200 from the 120 mg dry  $\text{kg}^{-1}$  soil  $\text{NH}_4^+\text{-N}$  (Figure 6a) regardless of rainfall immediately before some of the sampling  
201 sessions. Across the study period, the fluxes correlated log-linearly with soil  $\text{NH}_4^+$  content (Figure 6a). The DNDC  
202 model calculates  $\text{N}_2\text{O}$  fluxes driven by decomposition of organic N and denitrification following rainfall events  
203 (Li et al., 1992). However, more records of  $\text{N}_2\text{O}$  peaks after rainfall events are needed to feed a model properly.  
204 Our measured emissions were relatively high compared to the average  $31 \pm 22$   $\mu\text{g N}_2\text{O-N m}^{-2} \text{h}^{-1}$   
205 (average  $\pm$  standard deviation across studies) from the  $410 \pm 120$  mg dry  $\text{kg}^{-1}$  soil  $\text{NH}_4^+\text{-N}$  in Southeast Asian  
206 wetland forests (van Lent et al., 2015). Our measured fluxes were higher than model-predicted emissions of 21  
207  $\mu\text{g N m}^{-2} \text{h}^{-1}$  for the Amazon Basin (Guilhen et al., 2020) but agreed with huge  $\text{N}_2\text{O}$  emissions from floodplains  
208 soils of the Brazilian Amazon by Figueiredo et al. (2019).

(a) Swamp forest



(b) Manioc field



209

210 **Figure 6: Relationships between monthly average  $\text{N}_2\text{O}$  emission and soil N forms.**

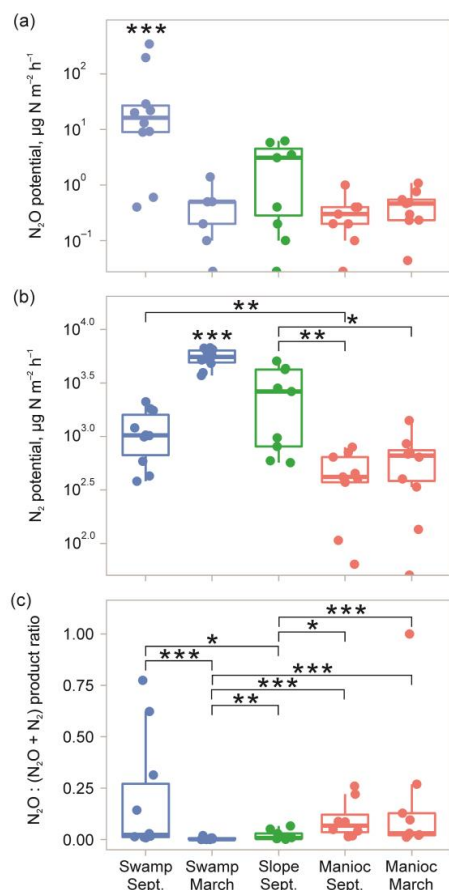




211 Soil  $\text{NO}_3^-$  content was below the detection limit in most of the anaerobic peat samples. This contradicts previous  
212 knowledge on low- $\text{NO}_3^-$  water-saturated peat as a negligible source of  $\text{N}_2\text{O}$  (Rubol et al., 2012; Teh et al., 2017;  
213 Pärn et al., 2018). However, Melillo et al. (2001) do report  $> 50 \mu\text{g N}_2\text{O-N m}^{-2} \text{ h}^{-1}$  in an Amazon rainforest  
214 peaking at low  $\text{NO}_3^-$  content. Most of anaerobic  $\text{N}_2\text{O}$  production pathways use  $\text{NO}_3^-$  as the source (Baggs, 2011;  
215 Butterbach-Bahl et al., 2013; Hu et al., 2015). Among the few exceptions, nitrifier denitrification avoids  $\text{NO}_3^-$   
216 reducing  $\text{NO}_2^-$  straight into  $\text{N}_2\text{O}$  (Wrage-Mönnig et al., 2018). Hergoualc'h et al. (2020) identified nitrifier  
217 denitrification in the palm swamp. It is a well-documented process in mineralised peats (Wrage-Mönnig et al.,  
218 2018; Masta et al., 2020). Anaerobic  $\text{NH}_4^+$  oxidation (anammox) involves nitric oxide (NO) as an intermediate  
219 product which could serve as an important substrate for  $\text{N}_2\text{O}$  formation by  $\text{NH}_4^+$  oxidisers or denitrifiers (Hu et  
220 al., 2015). Alternatively, co-denitrification reduces nitrogen dioxide ( $\text{NO}_2^-$ ) or NO into  $\text{N}_2\text{O}$  (Spott et al., 2011;  
221 Butterbach-Bahl et al., 2013). As another possible mechanism, the  $\text{O}_2$  supplied by aerenchymous palm roots (van  
222 Lent et al., 2019) may have driven incomplete nitrification with the derived  $\text{NO}_3^-$  immediately used up by plants  
223 and denitrifiers in heavy competition on the  $\text{NO}_3^-$  (Kuzuyakov and Xu, 2013). The latter in turn may have produced  
224 a part of the  $\text{N}_2\text{O}$  in the anaerobic soil zone (in agreement with van Lent et al., 2019). As a third potential source,  
225 we may consider denitrification in cryptogams such as lichens and fungi in other symbioses on the litter (Lenhart  
226 et al., 2015). The peat in our dry sites also emitted considerable  $43 \mu\text{g}$  (12 to  $55 \mu\text{g}$  as session average)  $\text{N}_2\text{O-N}$   
227  $\text{m}^{-2} \text{ h}^{-1}$  in a log-saturation curve relationship with soil  $\text{NO}_3^-$  content (Figures 5c, 6b).  
228 Across the sites, the potential  $\text{N}_2$  flow exceeded the potential  $\text{N}_2\text{O}$  flow by 1 to 2 orders of magnitude (Figure 7).  
229  $\text{N}_2\text{O}$  production potential in the intact soil cores collected from the Quistococha palm swamp forest after the  
230 September hot moment was  $64 \mu\text{g N m}^{-2} \text{ h}^{-1}$ . The soil cores collected in March and from other locations in all  
231 other sampling times showed near-zero  $\text{N}_2\text{O}$  production potential. The product potential of  $\text{N}_2$  in the palm swamp  
232 was  $1,100 \mu\text{g m}^{-2} \text{ h}^{-1}$  in late September and  $5,500 \mu\text{g m}^{-2} \text{ h}^{-1}$  in March. This shows that denitrification potential  
233 was deficient in September whereas in March practically all  $\text{N}_2\text{O}$  was converted to  $\text{N}_2$ . In the manioc field,  $\text{N}_2$   
234 production potential was low, further explaining the significant  $\text{N}_2\text{O}$  emissions (Figure 6b) with incomplete  
235 denitrification. In the toe-slope swamp forest,  $\text{N}_2$  potential was intermediate between the natural palm swamp and  
236 the manioc field, completing the clear  $\text{N}_2$  potential gradient according to the duration of the high water table.  
237



238 The field  $N_2O$  : ( $N_2O$  +  $N_2$  potential) product ratio was the highest at the Swamp in September, owing to huge  
 239  $N_2O$  emission and moderate  $N_2$  potential. These can probably be explained, again, by the water-table drawdown  
 240 and heavy shower before the sampling. In March the  $N_2O$  : ( $N_2O$  +  $N_2$ ) ratio showed near-zero values in the  
 241 Swamp, due to low  $N_2O$  emission and very high  $N_2$  potential. Thus, the  $N_2O$  likely produced from nitrifier  
 242 denitrification in March was consumed by denitrification. That likely resulted from the December rainfall after  
 243 which high water table settled in for months. The Slope also showed a low  $N_2O$  : ( $N_2O$  +  $N_2$ ) ratio owing to  
 244 moderate  $N_2O$  emission and high  $N_2$  potential. The  $N_2O$  : ( $N_2O$  +  $N_2$ ) ratio in the Manioc site was moderate, due  
 245 to moderate  $N_2O$  emissions and low  $N_2$  potential in the dry soil.



246  
 247 **Figure 7: Production potential of  $N_2O$  and  $N_2$  measured from intact soil cores, and product ratio of field-observed  $N_2O$**   
 248 **flux (Figures 5c and 6) to sum of field-observed  $N_2O$  flux and  $N_2$  production potential. Significant differences according**  
 249 **to Wilcoxon test are shown with asterisks as follows: \* –  $p < 0.05$ ; \*\* –  $p < 0.01$ ; \*\*\* –  $p < 0.001$ . Asterisks directly**  
 250 **above box without brackets denote significant difference from all other sites in the plot.**

251 Upscaling our  $N_2O$  measurements to the  $27,732 \pm 1,101 \text{ km}^2$  of palm swamp in the Pastaza-Marañon Basin  
 252 (Figure 2; Draper et al., 2014) yields  $30 \text{ Gg N yr}^{-1}$ . This constitutes roughly 2% of the  $1,300 \text{ Gg N yr}^{-1}$  from the  
 253  $5.4 \text{ million km}^2$  rainforest of the Amazon Basin (Melillo et al., 2001), a relatively small addition to the natural  
 254 fluxes, and emissions from land conversion, fertilisation and drainage (van Lent et al., 2015; Thompson et al.,  
 255 2019) in the biggest  $N_2O$  hotspot of the world (Figure 1; Ricaud et al., 2009). On the other hand, conversion of



256 the  $27,732 \pm 1,101$  km<sup>2</sup> of palm swamp in the Pastaza-Marañon Basin (Figure 2; Draper et al., 2014) to manioc  
257 fields could induce CO<sub>2</sub> emissions of 1.5 to 2.0 Tg C per month. This would add at least 4% to the current 1,500  
258 Tg CO<sub>2</sub> emission from Latin American land use (IPCC, 2019). Current Peruvian policy does not explicitly restrict  
259 agricultural development of peat swamps outside nature reserves and lands assigned to indigenous communities.  
260 Thus, a large share of the Peruvian peat carbon stocks is hanging on the isolation from population centres and low  
261 population density (Lilleskov et al., 2019).

## 262 Conclusions

263 The arable peatland in the Peruvian Amazon emitted relatively high amounts of CO<sub>2</sub> and N<sub>2</sub>O but the peat swamp  
264 forests under suppressed water table showed considerably larger CO<sub>2</sub> and N<sub>2</sub>O emissions while mostly retaining  
265 their naturally high CH<sub>4</sub> production. The likely mechanism behind the elevated GHG production was access of  
266 oxygen to the root zone. This caused high respiration and nitrifier denitrification while suppressing the full  
267 denitrification pathway. Further investigation is needed on the impact of global changes on the C and N stocks  
268 and cycles in tropical peatlands.

## 269 Acknowledgements

270 The study was supported by the Estonian Research Council (PRG352 and MOBERC-20 grants) and the EU  
271 through the European Regional Development Fund (ENVIRON and EcolChange Centres of Excellence, Estonia  
272 and the MOBTP101 returning researcher grant by the Mobilitas Plus programme), the European Social Fund  
273 (Doctoral School of Earth Sciences and Ecology), LIFE programme project “Demonstration of climate change  
274 mitigation potential of nutrients rich organic soils in Baltic States and Finland” (LIFE OrgBalt, LIFE18  
275 CCM/LV/001158), Czech Science Foundation (17-18112Y), and project SustES – Adaptation strategies for  
276 sustainable ecosystem services and food security under adverse environmental conditions  
277 (CZ.02.1.01/0.0/0.0/16\_019/0000797). Dr. Negron-Juarez was supported by the Next Generation Ecosystem  
278 Experiments – Tropics funded by the U.S Department of Energy, Office of Biological and Environmental  
279 Research. We would like to thank staff of the U. S. Department of Energy, U. S. Agency for International  
280 Development, U. S. Forest Service, University of Minnesota, University of Missouri, Michigan Technological  
281 University, Arizona State University, Oak Ridge National Laboratory, SilvaCarbon, Directorate of Foreign  
282 Commerce, Tourism and Crafts (DIRCETURA), Regional Government of Loreto (GORE-Loreto), and  
283 Quistococha Park for economic, managerial and scientific support.

## 284 References

- 285 Baggs, E. M.: Soil microbial sources of nitrous oxide: recent advances in knowledge, emerging challenges and future direction,  
286 *Current Opinion in Environmental Sustainability*, 3, 321-327, 2011.
- 287 Balogh, J., Pintér, K., Fóti, S., Cserhalmi, D., Papp, M., and Nagy, Z.: Dependence of soil respiration on soil moisture, clay  
288 content, soil organic matter, and CO<sub>2</sub> uptake in dry grasslands, *Soil Biology and Biochemistry*, 43, 1006-1013, 2011.
- 289 Butterbach-Bahl, K., Baggs, E. M., Dannemann, M., Kiese, R., and Zechmeister-Boltenstern, S.: Nitrous oxide emissions  
290 from soils: how well do we understand the processes and their controls?, *Philosophical Transactions of the Royal Society*  
291 *B: Biological Sciences*, 368, 2013.
- 292 Byrne, K. A., Kiely, G., and Leahy, P.: CO<sub>2</sub> fluxes in adjacent new and permanent temperate grasslands, *Agricultural and*  
293 *Forest Meteorology*, 135, 82-92, 2005.
- 294 Draper, F. C., Roucoux, K. H., Lawson, I. T., Mitchard, E. T. A., Honorio Coronado, E. N., Lähteenoja, O., Torres Montenegro,  
295 L., Valderrama Sandoval, E., Zarate, R., and Baker, T. R.: The distribution and amount of carbon in the largest peatland  
296 complex in Amazonia, *Environmental Research Letters*, 9, 124017, 2014.



- 297 Espenberg, M., Truu, M., Mander, Ü., Kasak, K., Nõlvak, H., Ligi, T., Oopkaup, K., Maddison, M., and Truu, J.: Differences  
298 in microbial community structure and nitrogen cycling in natural and drained tropical peatland soils, *Scientific Reports*, 8,  
299 4742, 2018.
- 300 Figueiredo, V., Pangala, S., Peacock, M., Gauci, V., Bastviken, D., and Enrich-Prast, A.: Contribution of trees to the N<sub>2</sub>O  
301 budget of Amazon floodplain forest, EGU General Assembly, Vienna, 2019.
- 302 Frolking, S., and Roulet, N. T.: Holocene radiative forcing impact of northern peatland carbon accumulation and methane  
303 emissions, *Global Change Biology*, 13, 1079-1088, 2007.
- 304 Granville, J.-J. d.: Aperçu sur la structure des pneumatophores de deux espèces des sols hydromorphes en Guyane: *Mauritia*  
305 *flexuosa* L. et *Euterpe oleracea* Mart. (*Palmae*). Généralisation au système respiratoire racinaire d'autres palmiers, *Cahiers*  
306 *ORSTOM. Série Biologie*, 3-22, 1974.
- 307 Griffis, T. J., Roman, D. T., Wood, J. D., Deventer, J., Fachin, L., Rengifo, J., Del Castillo, D., Lilleskov, E., Kolka, R.,  
308 Chimner, R. A., del Aguila-Pasquel, J., Wayson, C., Hergoualc'h, K., Baker, J. M., Cadillo-Quiroz, H., and Ricciuto, D.  
309 M.: Hydrometeorological sensitivities of net ecosystem carbon dioxide and methane exchange of an Amazonian palm  
310 swamp peatland, *Agricultural and Forest Meteorology*, 295, 108167, 2020.
- 311 Guilhen, J., Al Bitar, A., Sauvage, S., Parrens, M., Martinez, J. M., Abril, G., Moreira-Turcq, P., and Sánchez-Pérez, J. M.:  
312 Denitrification and associated nitrous oxide and carbon dioxide emissions from the Amazonian wetlands, *Biogeosciences*,  
313 17, 4297-4311, 2020.
- 314 Hergoualc'h, K., Dezzee, N., Verchot, L. V., Martius, C., van Lent, J., del Aguila-Pasquel, J., and López Gonzales, M.: Spatial  
315 and temporal variability of soil N<sub>2</sub>O and CH<sub>4</sub> fluxes along a degradation gradient in a palm swamp peat forest in the  
316 Peruvian Amazon, *Global Change Biology*, 26, 7198-7216, 2020.
- 317 Hu, H.-W., Chen, D., and He, J.-Z.: Microbial regulation of terrestrial nitrous oxide formation: understanding the biological  
318 pathways for emission rates, *FEMS Microbiology Reviews*, 39, 729-749, 2015.
- 319 Hubau, W., Lewis, S. L., Phillips, O. L., Affum-Baffoe, K., Bееckman, H., Cuní-Sánchez, A., Daniels, A. K., Ewango, C. E.  
320 N., Fauset, S., Mukinzi, J. M., Sheil, D., Sonké, B., Sullivan, M. J. P., Sunderland, T. C. H., Taedoung, H., Thomas, S. C.,  
321 White, L. J. T., Abernethy, K. A., Adu-Bredu, S., Amani, C. A., Baker, T. R., Banin, L. F., Baya, F., Begne, S. K.,  
322 Bennett, A. C., Benedet, F., Bitariho, R., Bocko, Y. E., Boeckx, P., Boundja, P., Brienen, R. J. W., Brncic, T., Chezeaux,  
323 E., Chuyong, G. B., Clark, C. J., Collins, M., Comiskey, J. A., Coomes, D. A., Dargie, G. C., de Haulleville, T., Kamdem,  
324 M. N. D., Doucet, J.-L., Esquivel-Muelbert, A., Feldpausch, T. R., Fofanah, A., Foli, E. G., Gilpin, M., Gloor, E.,  
325 Gonmadje, C., Gourlet-Fleury, S., Hall, J. S., Hamilton, A. C., Harris, D. J., Hart, T. B., Hockemba, M. B. N., Hladik, A.,  
326 Ifo, S. A., Jeffery, K. J., Jucker, T., Yakusu, E. K., Kearsley, E., Kenfack, D., Koch, A., Leal, M. E., Levesley, A., Lindsell,  
327 J. A., Lisingo, J., Lopez-Gonzalez, G., Lovett, J. C., Makana, J.-R., Malhi, Y., Marshall, A. R., Martin, J., Martin, E. H.,  
328 Mbayu, F. M., Medjibe, V. P., Mihindou, V., Mitchard, E. T. A., Moore, S., Munishi, P. K. T., Bengone, N. N., Ojo, L.,  
329 Ondo, F. E., Peh, K. S. H., Pickavance, G. C., Poulsen, A. D., Poulsen, J. R., Qie, L., Reitsma, J., Rovero, F., Swaine, M.  
330 D., Talbot, J., Taplin, J., Taylor, D. M., Thomas, D. W., Toirambe, B., Mukendi, J. T., Tuagben, D., Umunay, P. M., van  
331 der Heijden, G. M. F., Verbeeck, H., Vleminckx, J., Willcock, S., Wöll, H., Woods, J. T., and Zemağho, L.: Asynchronous  
332 carbon sink saturation in African and Amazonian tropical forests, *Nature*, 579, 80-87, 2020.
- 333 Hutchinson, G. L., and Livingston, G. P.: Use of chamber systems to measure trace gas fluxes, in: *Agricultural Ecosystem*  
334 *Effects on Trace Gases and Global Climate Change*, edited by: Harper, L. A., Mosier, A. R., Duxbury, J. M., Rolston, D.  
335 E., Peterson, G. A., Baenziger, P. S., Luxmoore, R. J., and Kral, D. M., 63-78, 1993.
- 336 Inatomi, M., Hajima, T., and Ito, A.: Fraction of nitrous oxide production in nitrification and its effect on total soil emission:  
337 A meta-analysis and global-scale sensitivity analysis using a process-based model, *PLOS ONE*, 14, e0219159, 2019.
- 338 IPCC: Land-climate interactions, in: *Climate Change and Land: an IPCC special report on climate change, desertification,*  
339 *land degradation, sustainable land management, food security, and greenhouse gas fluxes in terrestrial ecosystems*, edited  
340 by: P.R. Shukla, J. S., E. Calvo Buendia, V. Masson-Delmotte, H.-O. Pörtner, D.C. Roberts, P. Zhai, R. Slade, S. Connors,  
341 R. van Diemen, M. Ferrat, E. Haughey, S. Luz, S. Neogi, M. Pathak, J. Petzold, J. Portugal Pereira, P. Vyas, E. Huntley,  
342 K. Kissick, M. Belkacemi, J. Malley, In press, 2019.
- 343 Jauhainen, J., Silvennoinen, H., Hamalainen, R., Kusin, K., Limin, S., Raison, R. J., and Vasander, H.: Nitrous oxide fluxes  
344 from tropical peat with different disturbance history and management, *Biogeosciences*, 9, 1337-1350, 2012.
- 345 Karhu, K., Auffret, M. D., Dungait, J. A. J., Hopkins, D. W., Prosser, J. I., Singh, B. K., Subke, J.-A., Wookey, P. A., Ågren,  
346 G. I., Sebastià, M.-T., Gouriveau, F., Bergkvist, G., Meir, P., Nottingham, A. T., Salinas, N., and Hartley, I. P.:  
347 Temperature sensitivity of soil respiration rates enhanced by microbial community response, *Nature*, 513, 81-84, 2014.
- 348 Kuzyakov, Y., and Xu, X.: Competition between roots and microorganisms for nitrogen: mechanisms and ecological  
349 relevance, *New Phytologist*, 198, 656-669, 2013.
- 350 Leifeld, J., and Menichetti, L.: The underappreciated potential of peatlands in global climate change mitigation strategies,  
351 *Nature Communications*, 9, 1071, 2018.
- 352 Lenhart, K., Weber, B., Elbert, W., Steinkamp, J., Clough, T., Crutzen, P., Pöschl, U., and Keppler, F.: Nitrous oxide and  
353 methane emissions from cryptogamic covers, *Global Change Biology*, 21, 3889-3900, 2015.
- 354 van Lent, J., Hergoualc'h, K., and Verchot, L. V.: Reviews and syntheses: Soil N<sub>2</sub>O and NO emissions from land use and land-  
355 use change in the tropics and subtropics: a meta-analysis, *Biogeosciences*, 12, 7299-7313, 2015.
- 356 van Lent, J., Hergoualc'h, K., Verchot, L., Oenema, O., and van Groenigen, J. W.: Greenhouse gas emissions along a peat  
357 swamp forest degradation gradient in the Peruvian Amazon: soil moisture and palm roots effects, *Mitigation and*  
358 *Adaptation Strategies for Global Change*, 24, 625-643, 2019.
- 359 Li, C., Frolking, S., and Frolking, T. A.: A model of nitrous oxide evolution from soil driven by rainfall events: I. Model  
360 structure and sensitivity, *Journal of Geophysical Research: Atmospheres*, 97, 9759-9776, 1992.



- 361 Liengaard, L., Figueiredo, V., Markfoged, R., Revsbech, N. P., Nielsen, L. P., Prast, A. E., and Kühl, M.: Hot moments of  
362 N<sub>2</sub>O transformation and emission in tropical soils from the Pantanal and the Amazon (Brazil), *Soil Biology and*  
363 *Biochemistry*, 75, 26-36, 2014.
- 364 Lilleskov, E., McCullough, K., Hergoualc'h, K., del Castillo Torres, D., Chimner, R., Murdiyarso, D., Kolka, R., Bourgeau-  
365 Chavez, L., Hribljan, J., del Aguila Pasquel, J., and Wayson, C.: Is Indonesian peatland loss a cautionary tale for Peru? A  
366 two-country comparison of the magnitude and causes of tropical peatland degradation, *Mitigation and Adaptation*  
367 *Strategies for Global Change*, 24, 591-623, 2019.
- 368 Mander, Ü., Well, R., Weymann, D., Soosaar, K., Maddison, M., Kanal, A., Löhmus, K., Truu, J., Augustin, J., and Tournebize,  
369 J.: Isotopologue ratios of N<sub>2</sub>O and N<sub>2</sub> measurements underpin the importance of denitrification in differently N-loaded  
370 riparian alder forests, *Environmental Science & Technology*, 48, 11910-11918, 2014.
- 371 Melillo, J. M., Steudler, P. A., Feigl, B. J., Neill, C., Garcia, D., Piccolo, M. C., Cerri, C. C., and Tian, H.: Nitrous oxide  
372 emissions from forests and pastures of various ages in the Brazilian Amazon, *Journal of Geophysical Research:*  
373 *Atmospheres*, 106, 34179-34188, 2001.
- 374 Pangala, S. R., Enrich-Prast, A., Basso, L. S., Peixoto, R. B., Bastviken, D., Hornibrook, E. R. C., Gatti, L. V., Marotta, H.,  
375 Calazans, L. S. B., Sakuragui, C. M., Bastos, W. R., Malm, O., Gloor, E., Miller, J. B., and Gauci, V.: Large emissions  
376 from floodplain trees close the Amazon methane budget, *Nature*, 552, 230-234, 2017.
- 377 Pärn, J., Verhoeven, J. T. A., Butterbach-Bahl, K., Dise, N. B., Ullah, S., Aasa, A., Egorov, S., Espenberg, M., Järveoja, J.,  
378 Jauhainen, J., Kasak, K., Klemetsson, L., Kull, A., Laggoun-Défarge, F., Lapshina, E. D., Lohila, A., Löhmus, K.,  
379 Maddison, M., Mitsch, W. J., Müller, C., Niinemets, Ü., Osborne, B., Pae, T., Salm, J.-O., Sgouridis, F., Sohar, K., Soosaar,  
380 K., Storey, K., Teemusk, A., Tenywa, M. M., Tournebize, J., Truu, J., Veber, G., Villa, J. A., Zaw, S. S., and Mander, Ü.:  
381 Nitrogen-rich organic soils under warm well-drained conditions are global nitrous oxide emission hotspots, *Nature*  
382 *Communications*, 9, 1135, 2018.
- 383 Ricaud, P., Attié, J. L., Teyssèdre, H., El Amraoui, L., Peuch, V. H., Matricardi, M., and Schluessel, P.: Equatorial total column  
384 of nitrous oxide as measured by IASI on MetOp-A: implications for transport processes, *Atmospheric Chemistry and*  
385 *Physics*, 9, 3947-3956, 2009.
- 386 Roucoux, K. H., Lawson, I. T., Jones, T. D., Baker, T. R., Coronado, E. N. H., Gosling, W. D., and Lähteenoja, O.: Vegetation  
387 development in an Amazonian peatland, *Palaeogeogr., Palaeoclimatol., Palaeoecol.*, 374, 242-255, 2013.
- 388 Rubol, S., Silver, W. L., and Bellin, A.: Hydrologic control on redox and nitrogen dynamics in a peatland soil, *Science of the*  
389 *Total Environment*, 432, 37-46, 2012.
- 390 Ruwaimana, M., Anshari, G. Z., Silva, L. C., and Gavin, D. G.: The oldest extant tropical peatland in the world: a major carbon  
391 reservoir for at least 47 000 years, *Environmental Research Letters*, 15, 114027, 2020.
- 392 Ruzicka, J., and Hansen, E. H.: *Flow Injection Analysis*, J. Wiley & Sons, New York, 1981.
- 393 Schindler, T., Mander, Ü., Machacova, K., Espenberg, M., Krasnov, D., Escuer-Gatius, J., Veber, G., Pärn, J., and Soosaar,  
394 K.: Short-term flooding increases CH<sub>4</sub> and N<sub>2</sub>O emissions from trees in a riparian forest soil-stem continuum, *Scientific*  
395 *Reports*, 10, 3204, 2020.
- 396 Spott, O., Russow, R., and Stange, C. F.: Formation of hybrid N<sub>2</sub>O and hybrid N<sub>2</sub> due to codenitrification: First review of a  
397 barely considered process of microbially mediated N-nitrosation, *Soil Biology and Biochemistry*, 43, 1995-2011, 2011.
- 398 Teh, Y. A., Wayne, M., Berrio, J.-C., Boom, A., and Page, S. E.: Seasonal variability in methane and nitrous oxide fluxes from  
399 tropical peatlands in the western Amazon basin, *Biogeosciences*, 2017.
- 400 Thompson, R. L., Lassaletta, L., Patra, P. K., Wilson, C., Wells, K. C., Gressent, A., Koffi, E. N., Chipperfield, M. P.,  
401 Winiwarter, W., Davidson, E. A., Tian, H., and Canadell, J. G.: Acceleration of global N<sub>2</sub>O emissions seen from two  
402 decades of atmospheric inversion, *Nature Climate Change*, 9, 993-998, 2019.
- 403 Turetsky, M. R., Benscoter, B., Page, S., Rein, G., van der Werf, G. R., and Watts, A.: Global vulnerability of peatlands to  
404 fire and carbon loss, *Nature Geoscience*, 8, 11-14, 2015.
- 405 Wrage-Mönnig, N., Horn, M. A., Well, R., Müller, C., Velthof, G., and Oenema, O.: The role of nitrifier denitrification in the  
406 production of nitrous oxide revisited, *Soil Biology and Biochemistry*, 123, A3-A16, 2018.